OPEN ACCESS
Journal of Innovative Optical Health Sciences
Vol. 16, No. 2 (2023) 2230008 (17 pages)

DOI: 10.1142/S1793545822300087

World Scientific
www.worldscientific.com

Single-cell volumetric imaging with light field microscopy: Advances in systems and algorithms

Beibei Gao*, Lu Gao† and Fu Wang‡
School of Biomedical Engineering
Shanghai Jiao Tong University
Shanghai 200240, P. R. China
*gaobeibei919@sjtu.edu.cn
†lucy_gao@sjtu.edu.cn
‡wangfu@sjtu.edu.cn

Received 27 April 2022
Accepted 10 June 2022
Published 23 July 2022

Single-cell volumetric imaging is essential for researching individual characteristics of cells. As a nonscanning imaging technique, light field microscopy (LFM) is a critical tool to achieve real-time three-dimensional imaging with the advantage of single-shot. To address the inherent limits including nonuniform resolution and block-wise artifacts, various modified LFM strategies have been developed to provide new insights into the structural and functional information of cells. This review will introduce the principle and development of LFM, discuss the improved approaches based on hardware designs and 3D reconstruction algorithms, and present the applications in single-cell imaging.

Keywords: Light field microscopy; single-cell imaging; volumetric imaging; 3D reconstruction.

1. Introduction

Complex biological systems are composed of millions of cells. Single-cell imaging and analysis are fundamental to research biomedical mechanisms, which create a comprehensive understanding at the cellular level.[1,2] Two-dimensional single-cell imaging based on conventional wide-field fluorescence microscopy has been extensively employed to visualize the shape and detailed inner structures.[3,4] With the rapidly growing interest in the study of spatial information and interactions of cells, 3D microscopic imaging technology with high resolution, high speed and large field of view (FOV) is highly demanded.[5]

To acquire the 3D information of cells, the general imaging approach is to scan multiple planes of the biological sample. For example, point-scanning microscopy, such as confocal laser scanning microscopy (CLSM)[6] and multiphoton microscopy,[7] provides high-spatial resolution and optical sectioning at the expense of imaging speed and

‡Corresponding author.

potential photobleaching and phototoxicity in biological specimens. Alternatively, light-sheet microscopy, based on plane illumination, enables selective excitation of the focal plane with a thin laminar laser beam to reduce the background signal.[8,9] However, it relies on a series of individual images to build up a volume, which is inherently sequential. As an emerging scanning-free imaging technic, light field microscopy (LFM) has been extensively studied and applied in the biological field, benefiting from the capability of fast volumetric imaging.[10,11] In principle, LFM simultaneously collects both 2D spatial and 2D angular information of the incident light, and then computationally recovers the 3D information with single-shot imaging. Moreover, the configuration is simple and low-cost, which can be obtained only by some modifications on the traditional microscopy.[12,13] These advantages have driven the rapid development of LFM in recent years. Nevertheless, classical LFM suffers from compromised spatial resolution, uneven axial resolution and reconstruction artifacts near the native object plane (NOP). To solve these issues, a variety of advanced LFM modalities have evolved from the conventional LFM based on imaging system designs and volume reconstruction algorithms.

This review first introduces the principle and development of LFM techniques. Combining with the applications in single-cell 3D imaging, we then focus on the improved LFM imaging systems including wide-field LFM, light-sheet LFM and the integration with super-resolution microscopy techniques. Moreover, various volume reconstruction algorithms based on 3D deconvolution and deep learning will be discussed and analyzed. Lastly, we summarize the current technical challenges and future progress in LFM based on single-cell 3D imaging.

2. The Principle and Development

Light field imaging is a popular research field in computational photography. The light field can be modeled with a plenoptic function that is $L(x, y, z, \theta, \phi, \lambda, t)$,[14] describing the distribution of all light rays in free-space, where x, y and z are the space coordinates, θ and ϕ denote the angles, λ is the wavelength of light and t is the time. Due to the computational complexity of seven-dimensional (7D) plenoptic function, Levoy *et al.* simplified the 7D function and proposed a 4D light field model, i.e., $P(u, v, s, t)$.[15] Assuming two planes (u, v) and (s, t) that are not coplanar, the ray can be uniquely represented by the two intersections with these two planes, which contain 2D spatial information and 2D angular information. On this basis, an increasing number of advanced devices have been proposed to capture the light field images, including phase mask,[16] camera array[17] and microlens array (MLA).[18]

Based on the emerging light field imaging techniques, light field microscopy was originally introduced by Marc Levoy in 2006 (Fig. 1(b)).[10] They placed an array of microlenses in the native image plane (NIP) of conventional microscopy and then moved the camera to the rear focal plane of the MLA. Based on this, the spatial information can be collected by each microlens, and different angles or frequency information was captured by each sensor pixel behind the microlens so that raw light field image can be recorded. Practically, the f-number of the MLA must be matched to that of the objective to avoid overlapping or the waste of sensor space. Furthermore, considering that the focal length of MLA is usually a few millimeters, a 1:1 relay lens is required to project the back focal plane of the MLA onto the chip of sensor.[19] Then the algorithm such as tomography adopted by light field cameras can be employed to reconstruct a full volume.

It is worth noting that the extra angular information will lead to compromised spatial resolution, and the inevitable diffraction of microscopy makes the ray optics model inaccurate, which further degrades the spatial resolution. In 2013, Broxton proposed a wave optical model coupled with Richardson–Lucy (RL) deconvolution algorithm, which increased the resolution in LFM significantly.[20] However, further improvement of the image quality of LFM was hindered by two main factors. First, the point spread function (PSF) of the LFM was space-varying owing to different sampling information at different depths, consequently causing reconstruction artifacts, especially at the NOP. The second was high computational cost during the iterative deconvolution process due to multiple PSFs. To address these challenges, Fourier integral microscope (FLMic) was introduced with enhanced imaging performance and computational efficiency.[21] Instead of the native image plane, the MLA was transformed to the Fourier (pupil) plane of the objective using a Fourier lens (Fig. 1(c)). Each

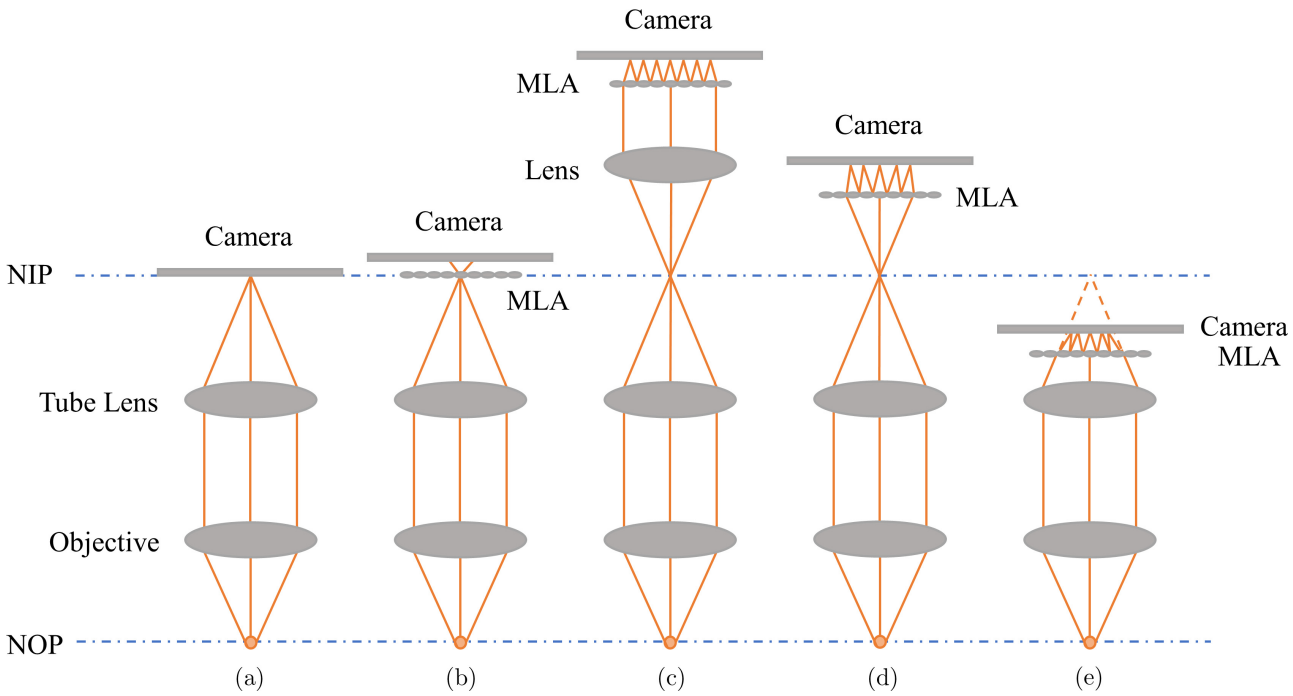

Fig. 1. Comparison of different imaging configurations: (a) wide-field microscopy; (b) conventional LFM; (c) Fourier LFM; (d) HR-LFM; (e) Gali-miniLFM.

microlens locally captured the light from different perspective angles and created a focused sub-image. With this method, the spatial-angular information can be recorded uncompromisingly, allowing spatially invariant sampling and reducing square artifacts. Similarly, Guo *et al.* derived a wave optical model that described the light propagation and volume reconstruction in Fourier light field microscopy (FLFM),[22] which was a high-potential technology in the realm of high-resolution single-cell imaging. Despite rapid progress of LFM, there is an unavoidable trade-off among different system characteristics such as temporal-spatial resolution, imaging speed and the field of view. In recent years, continuous efforts have been put forth to improve the imaging capability of LFM or FLFM, which will be discussed in Secs. 3 and 4 (Table 1).

3. Advanced Imaging Systems for LFM

In consideration of the inherent limits of classical LFM, growing interests have been focused on the improvement of hardware systems to provide advanced applications in single-cell 3D imaging including organelles, cytomembrane and the dynamic processes of live cells. Based on wide-field illumination mode, versatile LFM configurations with different modification solutions have been widely applied to observe and analyze the structures and interactions of organelles. In addition, diverse illumination approaches have emerged to enhance the imaging quality significantly. For instance, confocal LFM that implemented a generalized confocal detection scheme can effectively avoid the interference of out-of-focus fluorescence.[23] Using pseudorandom speckle produced by a spatial light modulator, the speckle LFM displayed high-resolution brain-wide volume imaging of neuronal activity with enhanced contrast.[24] In terms of the research of hemodynamics, light-sheet LFM with enhanced optical slicing capability has been a powerful imaging tool for investigating the cell flow with cellular resolution. Moreover, the integration of LFM and super-resolution microscopy provides the possibility to further enhance the resolution to nanometer-scale. We will discuss these advanced hardware systems and biomedical applications in detail in the following three sections.

3.1. *Wide-field light field microscopy*

Combining with wide-field illumination, multiple LFM strategies have been developed to enhance the resolution and signal-to-noise ratio, displaying

Table 1. Different LFM techniques for single-cell volumetric imaging.

System/Algorithm	Method[1]	Resolution ($x-y/\mu$m; z/μm)	Imaging volume size (μm^3)	Imaging rate (Hz)	Application	References
Wide-field LFM	Defocused LFM	< 1	Depth: $> 3\,\mu$m	> 100	Mitochondria	30
	HR-LFM	0.3–0.7/0.3–0.7	$> 133 \times 133 \times 3$	10	Golgi complex/Mitochondria	31
	HR-FLFM	0.3–0.7/0.5–1.5	$\sim 70 \times 70 \times 4$	50	Peroxisomes/Mitochondria	35
	hPSF-FLFM	2–3/5–6	$> 900 \times 900 \times 900$	100	Nucleic structures	37
	DAOSLIMIT	0.22/0.4	$225 \times 225 \times 16$	12	Migrasome dynamics	38
	MiSLFM	0.4/0.4	$90 \times 70 \times 70$	2	Membrane/Mitochondria/ Contractile vacuoles	41
Light-sheet LFM	Iso-LFM	$\sim 2.0 \pm 0.8/ \sim 2.91 \pm 0.2$	$\sim 300 \times 300 \times 300$	200	Blood cells tracking	42
	SVIM	$\sim 3/ \sim 6$	$440 \times 440 \times 100$	90	Blood cells tracking	48
	ASO-SVIM	$2.4 \pm 0.3/5.7 \pm 0.2$	$670 \times 470 \times 200$	50	Blood cells/Endocardium	49
	Hybrid light-sheet LFM	2/2	Depth: -76-76 μm	200	Myocardial contraction/Blood cells	51
Super-resolution LFM	SMLFM	0.02	$15 \times 15 \times 6$	—	Membrane	58
Richardson–Lucy	SPOT	0.8/1.6	—	—	Mitochondria	70
	SHVM	8.8/12.6	$\sim 1000 \times 1000 \times 500$	—	T cells/B cells	72
	DiLFM	—	$800 \times 600 \times 100$	100	Blood cells	96
Phase space	Phase space	—	—	—	B16 cell	83
	Low-rank prior	—	—	—	Neutrophil cell	87
	QLFM	1.8/2.5	$330 \times 330 \times 180$	25	Blood cells tracking	89
Deep-learning	DeepLFM	—	—	—	K562 cells	92
	VCD-LFM	1.1/3	$250 \times 250 \times 150$	200	Blood cells tracking	94

Notes: [1](1) HR-LFM: High-resolution LFM; (2) HR-FLFM: High-resolution Fourier LFM; (3) hPSF-FLFM: Hybrid point-spread function Fourier LFM; (4) DAOSLIMIT: Digital adaptive optics scanning light-field mutual iterative tomography; (5) MiSLFM: Mirror-enhanced scanning LFM; (6) Iso-LFM: Isotropic spatial resolution LFM; (7) SVIM: Light-field-based selective volume illumination microscopy; (8) ASO-SVIM: Single-objective SVIM; (9) SMLFM: Single molecule LFM; (10) SPOT: Snapshot projection optical tomography; (11) SHVM: Snapshot hyperspectral volumetric microscopy; (12) DiLFM: Dictionary LFM; (13) QLFM: Quantitative LFM; (14) DeepLFM: Deep learning-based LFM; (15) VCD-LFM: VCD neural network-based LFM.

superior performance in biomedical imaging. Especially, organelles embedded within the cytoplasm perform different functions for the natural operations of cells, which have been identified and analyzed widely using wide-field LFM. This section will provide an overview of diverse solutions for wide-field LFM, including the design of MLA, hybrid PSF and scanning LFM.

3.1.1. *LFM based on the design of MLA*

The image quality is influenced significantly by the parameters of MLA including the pitch, shape, focal length and position in the system. To increase the depth of field, a multifocal MLA was applied in a plenoptic camera,[25] which was an array of interleaved microlenses with different focal lengths. On this basis, Cong *et al.* introduced the multifocal imaging to a new extended field of view LFM (XLFM), enabling functional imaging of neural activity in larval zebrafish.[26] The 27 customized microlenses were divided into two groups with different focal planes that extended the working range. It should be noted that the system has not been employed for a variety of applications other than calcium imaging due to the lack of a computational framework for light propagation.

Original LFM fundamentally remains nonuniform resolution across multiple depths and prohibitive reconstruction artifacts owing to the depth-dependent sampling patterns. Defocused LFM system was designed by simply adjusting the MLA to a certain distance before or behind the NIP.[27,28] Similar to the Plenoptic 2.0 camera,[29] a defocused optical setup that shifted the MLA behind the NIP with a high-NA objective enabled high-resolution imaging.[30] The system recorded a $> 3\,\mu$m volume of mitochondria in HeLa cells with near-diffraction-limited resolution in three dimensions. Moreover, a high-resolution light field microscopy (HR-LFM) determined the distance values of NIP and sensor chip with numerical simulations to optimize the spatial-angular distribution (Fig. 1(d)).[31] With the configuration, the researchers exhibited the 3D imaging results of mitochondria and Golgi complex in fixed HeLa cells, showing well-resolved mitochondrial structures with a $\sim 3\,\mu$m axial range and Golgi structures with about 400 nm in all three dimensions. When observing the living-cell, a key challenge is how to decrease the photobleaching and photodamage. Using HR-LFM, the mitochondrial movements of $0.53\,\mu\mathrm{m\,s^{-1}}$ and occasional mitochondrial division were identified clearly with low light exposure (0.05–$0.5\,\mathrm{W\,cm^{-2}}$). Additionally, although Golgi-derived membrane vesicles in living COS-7 cells moved rapidly between the Golgi complex and other intracellular organelles sometimes, HR-LFM captured the rapid movement and interactions at a volume acquisition time of 0.01 s (Fig. 2(a)). Applying the same optical path design, a content-adaptive algorithm for the automatic correction of sCMOS-related noise (ACsN) was developed to minimize the readout noise of CMOS and sCMOS sensors.[32] The 3D reconstructed images of microtubules in a HeLa cell presented a significant improvement in the spatial resolution of cellular structures. Differing from HR-LFM, a novel optical system, called Galilean-mode light field miniscope (Gali-MiniLFM), was designed to place the MLA in front of the NIP so that the virtual native object plane was displaced to a deeper depth into the sample (Fig. 1(e)).[33] The Monte Carlo simulations illustrated the robustness in scattering tissue for imaging $10\,\mu$m fluorescent objects, while the anisotropic resolution and spatial-variant PSF still remained leading to expensive computational cost.

3.1.2. *LFM based on hybrid PSF*

For conventional LFM, the system generally depends on experimentally measured PSFs or numerical PSFs for volumetric reconstruction, which are susceptible to optical aberrations and block-wise artifacts. In 2021, a method named wFLFM with a hybrid wide-field image was developed by Liu and Jia.[34] The system was divided into two parts including wide-field imaging and light field imaging by a beam splitter. By displacing the low-resolution on-axis elemental images and upsampled FLFM PSF with wide-field images and focused wide-field PSF, respectively, it presented 2–3 times higher resolution compared with FLFM. Likewise, a hybrid PSF was proposed by Hua *et al.* to calibrate the deviation of calculated PSF, whose spatial positions were displaced by the experimental PSF results.[35] As the 3D-based *in vitro* cell culture system, organoids can be used to simulate the process of organogenesis and physiological and pathological states, which have broad application prospects in basic research and clinical diagnosis.[36] A hPSF-FLFM strategy that combined the on-axis

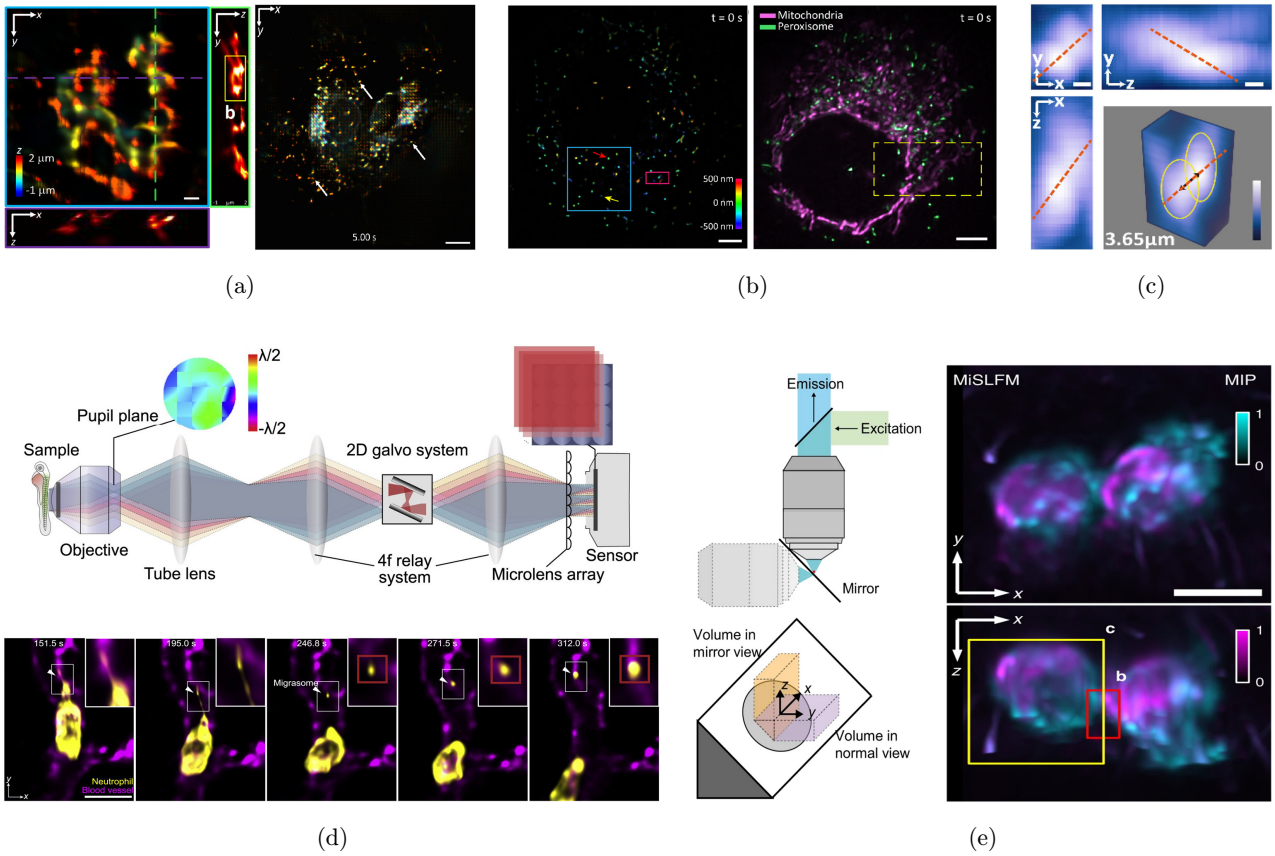

Fig. 2. Organelle imaging with wide-field LFM. (a) Imaging Golgi complex in HeLa cells (left) and Golgi-derived membrane vesicles in living COS-7 cells (right) using HR-LFM. Scale bars, 1 μm (left), 10 μm (right). Reproduced with permission from Ref. 31. (b) Imaging peroxisomes and mitochondria using HR-FLFM. Left: Reconstructed 3D image of peroxisomes. Right: Two-color stack projection of peroxisomes and mitochondria. Scale bar, 5 μm. Reproduced with permission from Ref. 35. (c) Nucleic structures in organoids using hPSF-FLFM. Scale bar, 2 μm. Reproduced with permission from Ref. 37. (d) Schematic of the sLFM system (top) and migrasome formation with gradually increasing fluorescence (bottom). Scale bar, 10 μm. Reproduced with permission from Ref. 38. (e) Objective and mirror configurations of MiSLFM (left) and MIPs of the reconstructed contractile vacuole (magenta, 488 nm) and cell membrane (cyan, 561 nm) (right). Scale bar, 10 μm. Reproduced with permission from Ref. 41.

numerical PSF and experimental PSF of the lateral location demonstrated excellent ability to visualize and analyze the organoids.[37] It was inspiring that the 3D individual cellular nuclei structures close to 3.65 μm have been identified clearly (Fig. 2(c)) and the fast response of single cell under the osmotic and mechanical stresses can be captured by the hPSF-FLFM system, which was expected to be an important imaging tool for the research of organoids.

3.1.3. *Scanning LFM*

Scanning LFM (sLFM) was first proposed by Wu *et al.*[38] They developed digital adaptive optics scanning light-field mutual iterative tomography (DAOSLIMIT) with the optical diffraction-limited resolution of 220 nm in the lateral and 400 nm in the axial direction at the millisecond level. In consideration of the contradiction between spatial resolution and angular resolution of wide-field LFM, DAOSLIMIT took advantage of the frequency coupling of multiple angles caused by the optical diffraction of MLA. Combining with high-speed periodic scanning of a galvanometer, the spatial overlap was introduced to preserve the high-frequency information at the cost of temporal resolution, thus obtaining high spatial and angular resolution simultaneously. Then a time-weighted algorithm based on spatio-temporal smoothness prior to biological samples was applied to decrease the motion artifacts and avoid the temporal resolution loss from scanning. In addition, DAOSLIMIT established a new framework for digital adaptive optics (DAO) imaging[39] to infer and correct the

aberrations according to the variation of angular components. With the unique capabilities of DAO-SLIMIT, the researchers carried out a series of experiments to study the dynamic process of migrasomes[40] in mammals (Fig. 2(d)). By labeling the neutrophils and vessels in the mouse liver, the generation and growth of migrasomes were recorded in detail. It was found that the migrasomes could be taken up by other neutrophils and their division abilities were potential for the information transferring in the immune system. When injecting the breast cancer cells into the zebrafish and mice, the process of vesicle split and migrasome production could be observed for a long time. However, the scanning LFM was restricted by the missing-cone problem. The result was that the axial resolution of the 3D reconstruction was lost and much lower than the lateral resolution.

To address the limit, Xiong *et al.* further developed the sLFM scheme and introduced a mirror-enhanced scanning light-field microscopy, MiSLFM.[41] An additional mirror was implemented below the sample to collect twice as many photons with only half of the laser intensity. Then in combination with phase-space deconvolution algorithm, high-isotropic-resolution 3D imaging of $\sim 400\,\text{nm}$ with high speed and low phototoxicity could be achieved. Using the configuration, B16-GFP live cells were observed with $0.22\,\text{mW}\,\text{mm}^{-2}$ illumination density lasting $\sim 14\,\text{h}$, while confocal microscopy only kept for 3 h. Furthermore, the contractile vacuoles and membrane of Dictyostelium discoideum can be identified with improved axial resolution, demonstrating the excellent ability of imaging fast-moving biological samples (Fig. 2(e)). However, the expense of improved axial resolution was the reduced field of view and degraded resolution at the edge of imaging, which can be addressed with multiple objective lenses.[42]

3.2. *Light-sheet light field microscopy*

Classical LFM employing wide-field illumination suffers from the background interference beyond the volume of interest, consequently constraining the contrast of the reconstructed 3D image. Alternatively, in light-sheet microscopy, also termed single plane illumination microscopy (SPIM), excitation light is shaped into a plane beam perpendicular to the detection objective. Individual slices are recorded in parallel with the thin laminar light to block out-of-focus light, permitting high-speed 3D optical sectioning.[43] By integrating the benefits of light sheet illumination with LFM, the novel hybrid optical configuration potentially allows fast acquisition of volumetric information with limited background noise.

Considering that the progressive hybrid system remained complicated and nontrivial to design and build, a comprehensive guide was provided including the selection of the optical components and a detailed design workflow.[19] Based on a digital micromirror device (DMD), Wolff *et al.* presented a three-time improvement of axial resolution from about $1.5\,\mu\text{m}$ to about $4.5\,\mu\text{m}$, yet sacrificing the time resolution about three times. Moreover, when the DMD redirected and formed the excitation light, most of the pixels of DMD were in the off state leading to a great waste of light power.[44] Differing from DMD, a hybrid light-sheet light-field microscopy (LSLFM) system was designed to generate the static excitation light-sheet by a cylindrical lens and scan the plane light with a 1D galvo mirror, making the illumination more efficient (Fig. 3(a)).[45] The researchers designed and implemented a switchable and versatile platform that integrated three different modalities including wide-field LFM, light-sheet microscopy and the proposed LSLFM method. The platform can acquire the images for light-sheet microscopy and LSLFM simultaneously benefiting from the same light-sheet excitation source. For wide-field LFM, a light-emitting diode was employed for illumination. The imaging results of fluorescent beads and live zebrafish demonstrated a 10-fold improvement in contrast and a 3.2-fold signal-to-noise ratio (SNR) of wide-field illumination. It was worth noting that the additional artifacts could degrade the image quality caused by the scattering and absorption of samples from the plane light.

In the field of single-cell imaging, the significance of 3D imaging for living cells lies more in the ability to monitor the kinetic process over a longer period.[46,47] In recent years, various attempts based on light-sheet light field microscopy techniques have been made to explore the blood flow including cardiac hemodynamics and cerebral hemodynamics. In 2019, Wagner *et al.* presented a creative isotropic spatial resolution light-field microscopy (Iso-LFM) based on dual-view imaging system (Fig. 3(b)).[42] Combining the specific advantages of selective-volume illumination and light field collection, two

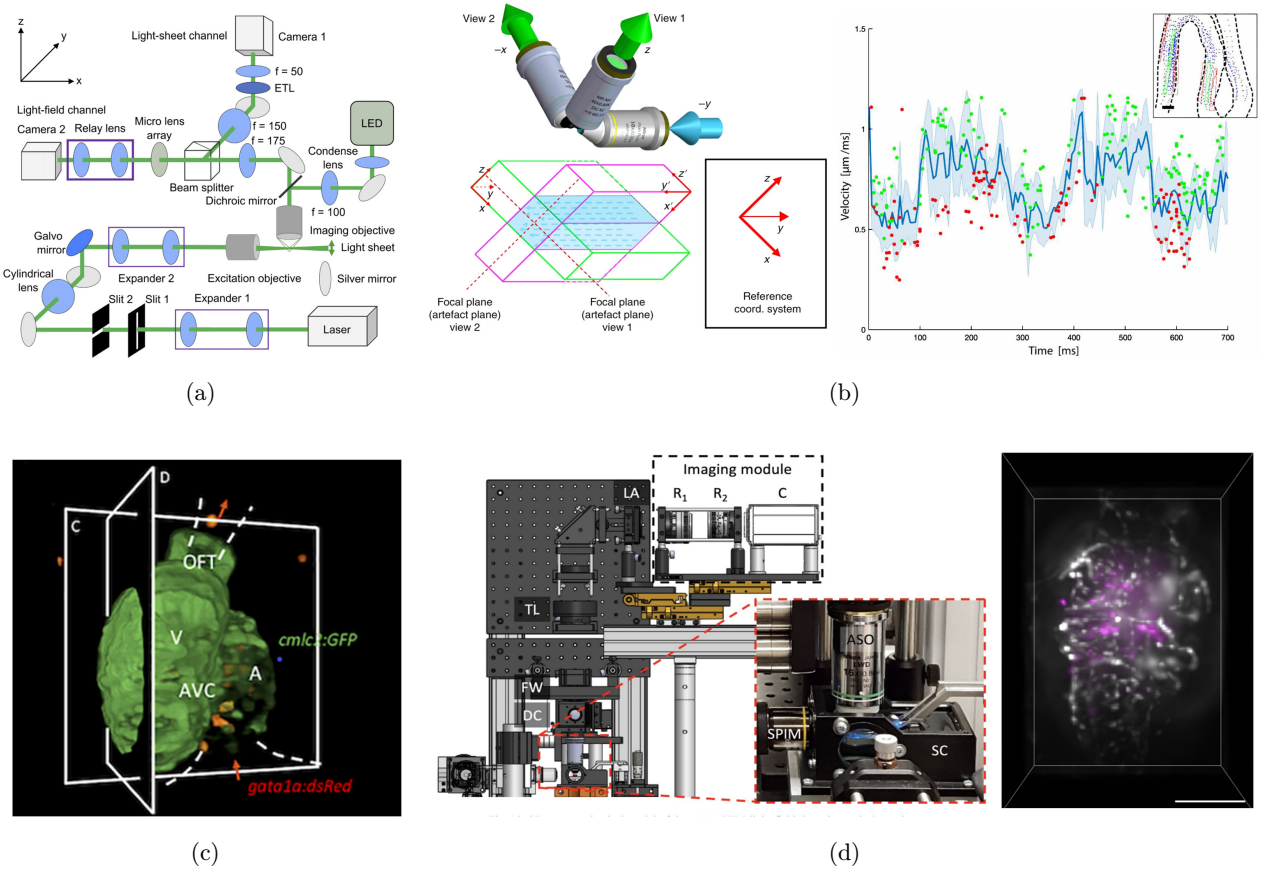

Fig. 3. Blood cell imaging and tracking with light-sheet LFM. (a) Conceptual schematics of LSLFM. Reproduced with permission from Ref. 45. (b) Objective configuration of Iso-LFM (left) and blood flow quantifications from single-cell tracking (right). Reproduced with permission from Ref. 42. (c) Imaging GFP-labeled cardiomyocyte light chain and DsRed-labeled blood cells in an embryonic heart. Scale bar, 50 μm. Reproduced with permission from Ref. 51. (d) 3D mechanical structure of detection path for ASO-SVIM (left) and imaging whole-brain blood flow in zebrafish larvae (right). Scale bar, 100 μm. Reproduced with permission from Ref. 49.

detection objectives were installed orthogonally, perpendicular to the illumination objective and two MLA were arranged at the native image plane of the two detective objectives, respectively. It was inspiring that the spatial resolution was uniform and there were no motion blur artifacts benefiting from the simultaneous illumination and recording of two light fields. These characteristics played a significant role in the imaging and analysis of fast blood flow, potentially driving the rapid development of hemodynamics. Using the scheme, the researchers presented *in vivo* imaging of the beating heart in the juvenile medaka fish. The cardiomyocytes were observed in the volume FOV range of $\sim 300 \times 300 \times 300\,\mu m^3$ at a volume rate of 143 Hz, and the cardiomyocyte nuclei could be identified clearly with single-cell resolution. Then they tracked the undiluted eGFP-labeled circulating blood cells in the cardiovascular system at up to $1400\,\mu m\,s^{-1}$ while the classical LFM performed poorly due to the low resolution. Despite its superior performance, the expanded laser beam of 100 μm was used to completely fill the volume of interest without scanning, which could generate blurred boundaries. Alternatively, a confined excitation beam of $\sim 5\,\mu$m was chosen by light-field-based selective volume illumination microscopy (SVIM) achieving better spatial precision.[48] There were two excitation modes via 1p (one-photon) continuous-wave lasers and 2p (two-photon) femtosecond-pulsed lasers. Two objectives that were perpendicular to each other were implemented for selective illumination and light field capture separately. When imaging the live beating heart of a $\sim 250 \times 150 \times 150\,\mu m^3$ zebrafish larva at 90 volumes s^{-1}, SVIM outperformed wide-field LFM with 50% better contrast of motions of the beating heart wall and 10% of moving blood cells. However,

the volume-scanning approach made the whole system complicated and restricted the size of the sample. Based on this, a modified configuration termed axial single-objective SVIM (ASO-SVIM) was further proposed by the research team.[49] The system implemented a unique objective with high NA to decrease the system complexity. Instead of lateral illumination, one-photon excitation (1P-ASO-SVIM) employed a cylindrical lens to tilt the light sheet illumination plane in 1D scanning. For two-photon, a near-infrared Gaussian beam was raster-scanned in 2D increasing the imaging depth. As a result, two-color imaging of blood cells and endocardium in the whole-brain blood flow of zebrafish larvae with $\sim 670 \times 470 \times 200\,\mu m^3$ volume at ~ 50 Hz demonstrated improved resolution and contrast (Fig. 3(d)). In addition, together with retrospective gating method,[50] Wang *et al.* captured myocardial contraction and the motion of single blood cell at about 200 Hz, thereby contributing to the development of the cardiac mechanics (Fig. 3(c)).[51] We anticipate light-sheet light field microscopy to provide a promising paradigm for the investigation of complex cardiac hemodynamics and cerebral hemodynamics at the cellular level.

3.3. *LFM combined with super-resolution microscopy techniques*

Super-resolution microscopy can offer the visualization of the previously unobserved nanoscale structures by bypassing the resolution limitation of optical diffraction.[52] After more than two decades of development, it has evolved to be a predominant tool for exploring the inner structure of single cells.[53,54] In recent years, several novel approaches that combined super-resolution microscopy with LFM have been verified to enhance the spatial resolution of 3D imaging, even up to the nanoscale.

One of the super-resolution imaging techniques is structured illumination microscopy (SIM).[55] By designing the spatial structure of the illumination light, the high-frequency information can be shifted to the visible low-pass band of the microscopy. Then a specific algorithm can be employed to separate the high-frequency components to reconstruct a super-resolution image. Inspired by the advanced SIM, a structured-illumination light-field microscopy (SI-LFM) was proposed, yielding a high-resolution and high-speed 3D imaging configuration.[56] The researchers implemented a DMD to generate depth invariant structured pattern with a super-pixel approach (Fig. 4(a)). Then a light field reconstruction approach for raw light field images refocusing and a SIM reconstruction strategy to obtain high-frequency information worked together to achieve high-resolution volumetric imaging. Moreover, Fu *et al.* introduced the light-sheet illumination to the structured light illumination light field microscopy, termed SLI-LFM,[57] at the imaging field of view of $250 \times 250 \times 80\,\mu m^3$ with high SNR. A polygonal scanner and a galvanometer scanned the plane light-sheet horizontally and vertically separately. With two exposures, two light field images with uniform and sinusoidal pattern illumination generated by DMD were captured successively. Then, they proposed a reconstruction model integrating deconvolution with the HiLo algorithm to realize a 1.3-fold enhancement of axial resolution compared with light sheet LFM, whereas the lateral resolution remained limited and the issues of artifacts at the focal plane were still unsolved.

An alternative approach was single molecule light field microscopy (SMLFM)[58] that can image the single fluorophore from multiple angles with the advantage of aperture segmentation characteristic of MLA (Fig. 4(b)). The square lattice MLA was placed at the Fourier plane to build a FLFM system and then the 3D localization model was established with a linear equation of $Ax = b$, where A represented the localization difference from diverse perspective views and b was the set of 2D localizations for a single emitter. The focal length of the lens that was placed in a 4f configuration with a tube lens determined the maximum precision and depth-of-field of imaging system. Therefore, two achromatic lenses of 75 mm (configuration 1) and 100 mm (configuration 2) were implemented, respectively, to obtain different number of illuminated microlenses and magnification. The researchers displayed the test results of 100 nm fluorescent beads. Using 4000 emitted photons on average, both configurations obtained isotropic lateral and axial precision, which remained below 20 nm in the depth range of $3\,\mu m$. When imaging the membrane of T cells, up to 25 light field localizations per frame were presented (Fig. 4(c)). The system was significantly promising for the multicolor imaging of membrane contour and microvilli. However, SMLFM suffered from a limited imaging field of view of $15 \times 15\,\mu m^2$ and low

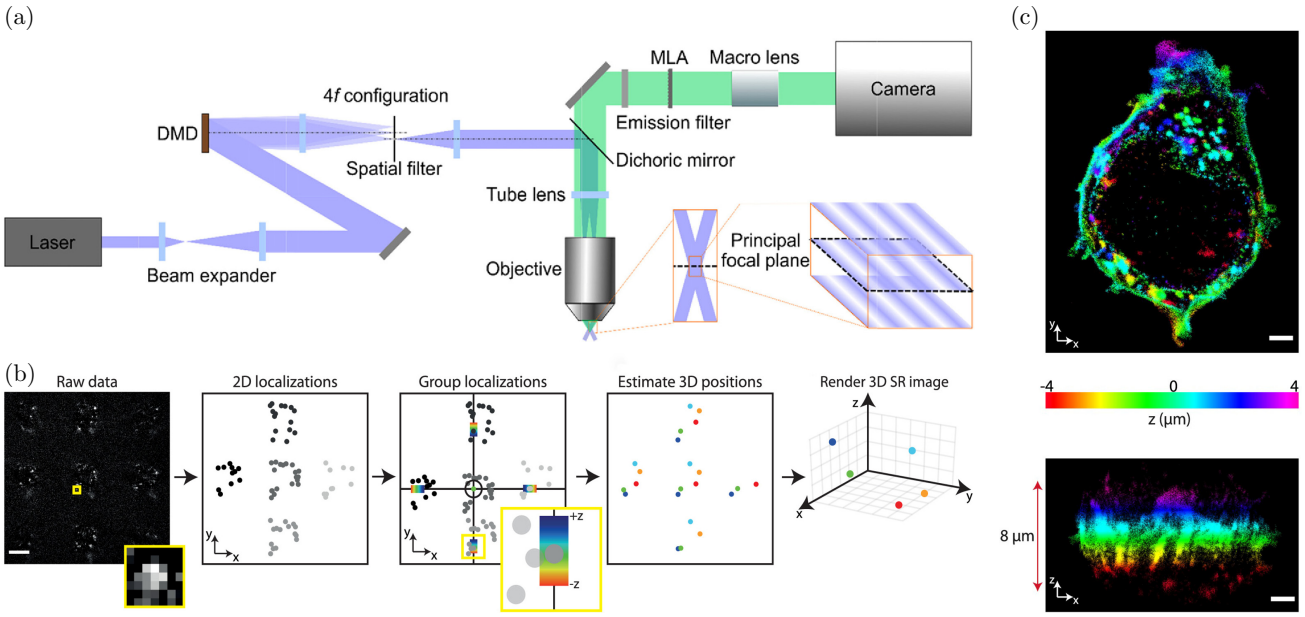

Fig. 4. Imaging membrane using LFM based on super-resolution microscopy. (a) Schematic of SI-LFM. Reproduced with permission from Ref. 56. (b) 3D emitter position estimation algorithm of SMLFM. (c) Imaging membrane of fixed Jurkat T-cells using SMLFM. Scale bar, 2 μm. (b) and (c) were reproduced with permission from Ref. 58.

photon utilization efficiency. Therefore, further advancements in super-resolution LFM to achieve nanometer-scale resolution and rapid 3D imaging with larger FOV are highly desirable to explore.

4. 3D Reconstruction Algorithms for LFM

After capturing the raw light field images, a robust reconstruction algorithm is expected to achieve a high-resolution 3D image. In particular, observing the dynamic process of interactions between different organelles in living cells necessitate excellent imaging algorithms over relatively short timescales.[59] Taking inspiration from photography, a great number of advanced methods have been proposed based on ray-optics model.[60,61] Light field depth estimation method including epipolar plane image (EPI) method[62] and refocusing-based method,[63] originally proposed from photography, is to obtain scene depth information using different features of the light field. On this basis, combining the EPI method and light field back projection (LFBP) reconstruction algorithm, a light field light-sheet fluorescence microscopy enhanced the depth resolution to be less than 0.5 μm without the sacrifice of spatial resolution.[64] In addition, Shaw *et al.* integrated the depth estimation approach of refocusing into light field microscopy to observe and quantify the 3D body shape and movement characteristics of moving C. elegans.[65] Nevertheless, the approaches based on photography remain restricted by the intrinsic diffraction of light microscopy, causing much inaccuracy in the light ray model. Alternatively, 3D deconvolution algorithms based on wave-optical model and deep learning without an accurate mathematical model have been widely applied to the 3D reconstruction of LFM, which can enhance the spatial resolution significantly and eliminate the artifacts simultaneously. As expected, both two methods have fulfilled the potential in studying the internal structure and dynamic process of single cell.

4.1. *3D deconvolution-based reconstruction*

3D deconvolution is an operation to recover three-dimensional volume from raw images which are resolution-limited and corrupted by noise.[66,67] Particularly, RL deconvolution was initially proposed for LFM in 2013[20] and then various modified LFM based on RL algorithms have exhibited appealing performance on single-cell imaging. For example, Prevedel *et al.* observed the dynamic activity of neuronal cells with high spatial and

temporal resolution.[68] Quicke *et al.* presented somatic and dendritic structures by 3D subcellular GEVI imaging.[69] Sung *et al.* imaged the mitochondria localized of a bovine pulmonary artery endothelial (BPAE) cell, showing the great ability of optical section.[70] In 2021, a high-resolution Fourier light-field microscopy (HR-FLFM) was developed to explore the inner organelles of living cells for a long time continuously.[35] In conjunction with the RL approach and 3D PSF, HR-FLFM retrieved the volume information of the sample by 20–50 iterations within 4 to 9 s. As a result, the 3D structures of immuno-stained mitochondria in COS-7 cells were recorded with a near-diffraction-limited resolution. In addition, two-color imaging of GFP-labeled peroxisomes and MitoTracker-labeled mitochondria exhibited the relative locations and dynamic interactions of the two organelles for 30 s (Fig. 2(b)). The results showed that the peroxisomes distributed over a depth range of 1.5 μm were interspersed in the mitochondrial voids with 3–4 μm thickness.

Although the RL algorithm has achieved great success, 3D reconstruction from captured raw light field images is considered as an ill-posed inverse task restricted by several unavoidable barriers. The iterative RL algorithm suffers from vast calculating amount and strong artifacts near the NOP due to space-variant PSF. To address the problems, a series of modifications to the RL approach have been exploited to facilitate the image quality of 3D reconstruction. Zheng *et al.* obtained the loss function through KL divergence of the Poisson noise likelihood to achieve isotropic spatial resolution.[71] Wu *et al.* presented a snapshot hyperspectral volumetric microscopy (SHVM) with a creative 4D deconvolution algorithm to record hyperspectral volumetric data.[72] By combining the expectation maximization (EM) method[73] with the total variation (TV) regularization[74] and utilizing the sparse prior of fluorescent objects, the 4D deconvolution contributed to increase the imaging speed significantly. Using the scheme, the location of T cells and B cells and the motion of T cells in lymph node can be identified clearly. Furthermore, to mitigate artifacts, the total variation (TV) regularization was also used by Stefanoiu *et al.* for image denoising in FLFM.[75] Based on the conventional maximum likelihood expectation maximization (MLEM) algorithm, the researchers introduced the penalized likelihood[76] method to update each iteration of deconvolution. While for the novel 3D reconstruction strategy proposed by Verinaz-Jadan *et al.*,[77] the result of TV regularization was not consistent with the experimental result. Therefore, an alternating direction method of multipliers (ADMM) optimization strategy[78] was chosen for minimizing artifacts. They proposed an optimized forward model, which employed a generating function to compute the system response. Additionally, Stefanoiu *et al.* proposed an anti-aliasing filtering approach to all the LFM systems.[27] The researchers first analyzed the depth-related sampling patterns and the cause of producing artifacts and then proposed a generalized light field point spread function based on wave optical. For the 3D deconvolution, an additional anti-aliasing filter using a Lanczos2 windowed version of the sinc kernel was added for every iteration of RL method. The imaging results of a cardiomyocyte organoid at the depth of 0 to 50 μm showed the higher resolved features without strong artifacts in comparison with original RL algorithm. Nevertheless, all of the above-mentioned approaches remained restricted from noise when observing the biological samples sensitive to phototoxicity. A dictionary LFM (DiLFM) was presented to remove a series of reconstructed artifacts and thus can facilitate the imaging performance at extremely low illumination level remarkably (Fig. 5(a)).[96] First, a few iterations of RL were used to obtain raw reconstruction volume affected by harsh background interference and artifacts. Then a pair of low- and high-fidelity dictionaries were trained to replace the matched poor RL reconstructions with high-quality elements. By introducing different scales of noise interference, the DiLFM could further learn the impact of noise to construct robust compensation.[79] The imaging results of zebrafish blood cells at 100 Hz with 0.12 mW illumination power displayed more detailed structures of blood cells and blood vessel walls compared with classical LFM.

Besides the RL algorithm, several methods based on sparsity priors have achieved great reconstruction performance, but they were limited to neuronal activity.[80–82] Alternatively, a phase-space approach was developed to eliminate the block-wise artifacts close to the NOP and enhance the speed of convergence during the deconvolution process (Fig. 5(b)).[83] The angular components were realigned in the phase space, where the PSF was spatial-invariant avoiding the periodic artifacts and excessive iterations. Then utilizing the smooth

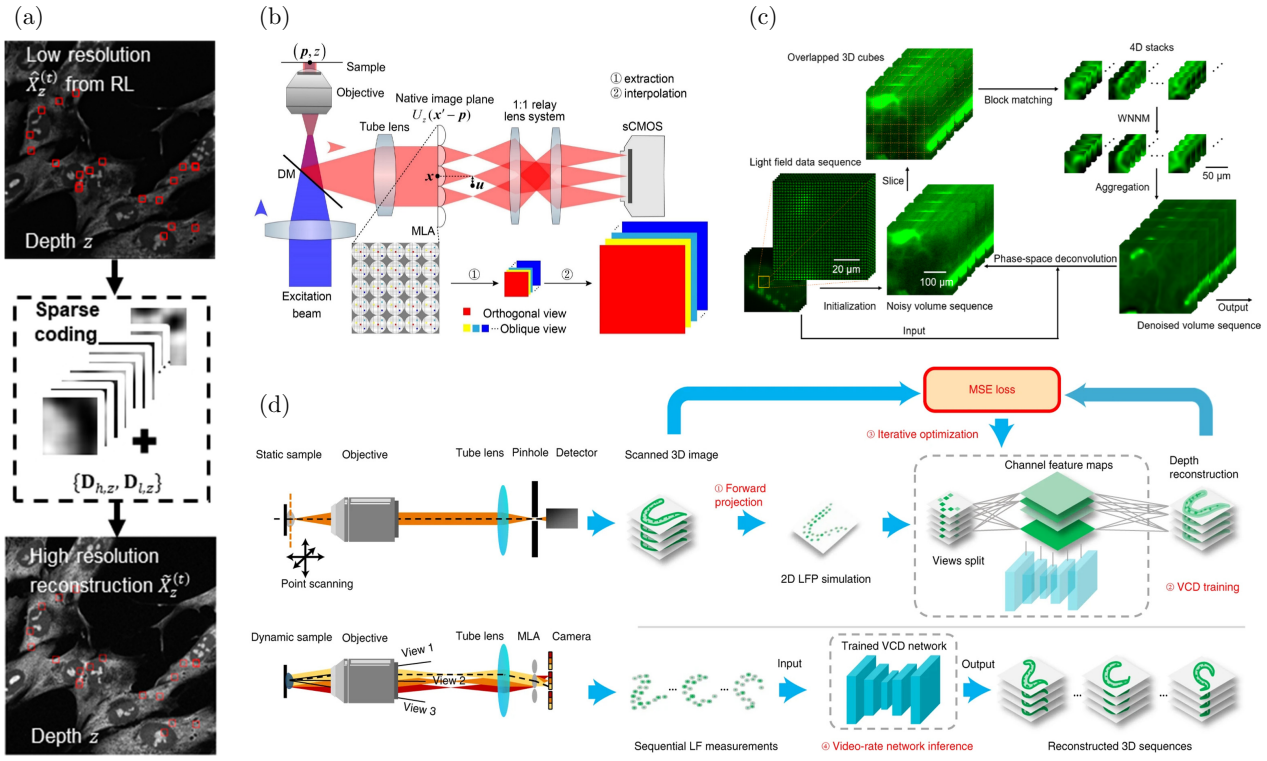

Fig. 5. Principles of different 3D reconstruction algorithms. (a) Procedure of DiLFM. Reproduced with permission from Ref. 96. (b) Schematic of phase-space deconvolution. Reproduced with permission from Ref. 83. (c) Framework of spatial-temporal low-rank prior in phase-space deconvolution. Reproduced with permission from Ref. 87. (d) Framework of VCD-net for stationary samples using confocal microscope (top) and dynamic samples using light field microscopy (bottom). Reproduced with permission from Ref. 94.

constraint,[84] a cubic interpolation[85] for up-sampling was applied to improve the resolution. The researchers imaged the GFP-labeled B16 cell, which exhibited more subcellular structures and fewer artifacts while the results of conventional RL algorithm with 2 iterations and 20 iterations both showed low contrast. On this basis, Xiong *et al.* introduced the phase-space deconvolution into mirror-enhanced scanning LFM,[41] enhancing the resolution to the diffraction-limit. In consideration of low SNR and heavy computational complexity of the original phase-space deconvolution, the spatial-temporal low-rank prior with weighted nuclear norm minimization (WNNM) denoising[86] was introduced, which enabled the volume reconstruction of neutrophil cells in the weak illumination condition with high SNR (Fig. 5(c)).[87] When imaging the biological samples, inherent scattering and dense fluorescence labeling degraded the image quality inevitably.[88] Zhang *et al.* developed a multiscale model in the phase-space to observe the movement track of blood cells of zebrafish larvae with high resolution.[89] However, affected by the missing-cone problem, this model suffered from lower axial resolution compared with confocal microscopy, which could be settled with super-resolution technology.

4.2. *Deep-learning-based reconstruction*

Even though 3D deconvolution has realized high-resolution volume reconstruction, these methods still rely on precise mathematical light propagation model and complex point spread function, prone to be affected by system errors and experimental conditions. Alternatively, the emerging deep learning methods have been incorporated into LFM, which can obtain 3D volume from raw light field images directly, improving the reconstruction speed significantly.[90,91] In 2019, a DeepLFM was presented to reconstruct 3D images of K562 cells with higher-spatial resolution than RL algorithm.[92] After 10 iterations of RL deconvolution, a 3D U-net[93] was applied to super-resolve the low resolution deconvolved 3D volume. However, several iterations brought extra computation requirements, and

consequently limited the imaging speed. In contrast, the modified U-net was used in a view-channel-depth network (VCD-Net) that removed the RL procedure to provide a direct bridge between the raw light field images and reconstruction results (Fig. 5(d)).[94] With the advantages of high speed and isotropic spatial resolution, the researchers successfully achieved the 3D volume of cardiomyocytes and blood cells at a 200-Hz volumetric imaging rate. Instead of simulated data in VCD-Net, the train data of LFM-Net was obtained from real LFM images so that the optical characteristics can be learned as prior knowledge.[95] The network exhibited excellent reconstruction volume with accuracy similar to that of confocal imaging and enhanced 720-fold imaging speed coupled with 1/64 storage space. Undoubtedly, the fast-evolving deep learning technology will further expand the imaging performance and application field of LFM.

5. Conclusions and Outlook

In the last decade, LFM for single-cell 3D imaging has received significant attention and provided new insights into the inner structures and biomechanical characteristics of single cell, due to the remarkable capability of capturing volume information by a single-shot. Despite superior performance, LFM remains suffering from compromised resolution and strong artifacts owing to the segmentation of MLA. This paper presented a brief review of the enhancement of LFM on the hardware systems and 3D reconstruction algorithms and introduced the latest applications in single-cell imaging using improved LFM strategies.

Current LFM implements mainly have several challenges: (1) inherent trade-off between spatial resolution and angular resolution; (2) inevitable block-wise artifacts near the native object image; (3) high demands on computation resources caused by space-variant PSF; (4) low SNR interfered by background fluorescence. To mitigate these restrictions, various strategies based on system designs or reconstruction algorithms have emerged, leading to greater advancements in single-cell volumetric imaging. For compromised spatial resolution, a more accurate light propagation model contributes to higher quality reconstruction volume. Furthermore, integrating the super-resolution techniques with LFM such as SMLM or SIM is expected to achieve nanometer-scale resolution. In terms of severe artifacts, FLFM that shifts the position of MLA and phase space that realigns the angular information are both optional methods to avoid the artifacts close to NOP. According to sLFM, the aberration can be calibrated remarkably benefiting from advanced adaptive optics. Additionally, high computation cost can be effectively reduced through simplified light model with prior knowledge and fast-developed deep learning methods, which can improve the reconstruction speed dramatically. Lastly, a hybrid microscopy system that combines the different illumination modes including confocal and light-sheet can offer notable contrast improvement.

Despite substantial progress in the area of LFM, the spatial-temporal resolution and imaging volume still mutually restrict each other. As shown in Table 1, the improved methods and corresponding performance are summarized for a better comparison. To maximize the strengths of LFM system in the field of single-cell imaging, appropriate illumination modes, reconstruction algorithm and experiment samples need to be considered carefully according to the research requirements. When imaging the subcellular structures and dynamics of organelles such as mitochondria and Golgi complex, wide-field LFM can present better spatial resolution in spite of lower imaging volume. And the integration of super-resolution microscopy can enhance the resolution to nanometer-scale. For the research of cardiac hemodynamics and cerebral hemodynamics, light-sheet LFM with deep-learning technology is a valuable tool due to reduced background noise and efficient data processing, which contributes to tracking the motion of single blood cell in live embryos at a video time.

In the future, we expect that the developed light field microscopy techniques will further provide more valuable structural and functional information of single cell. First, it is necessary to continue to push the spatial resolution and computation efficiency, which can be facilitated with more sensitive sensors, robust reconstruction algorithms and faster GPU processing. Furthermore, deeper penetration depth still remains limited. Therefore, continuous efforts are expected to achieve larger FOV without the degradation of resolution. Certainly, the development of novel near-infrared imaging systems and fluorophores will provide the possibility of imaging depth improvement. For the applications of single-cell imaging, visualizing directly the subcellular

interactions and conformations inside cells remains a challenging task for LFM. In addition, the exploration of cardiac hemodynamics and cerebral hemodynamics at the cellular level proposes high requirements for LFM with real-time high-resolution imaging. Hopefully, with the progress of various imaging techniques such as multiphoton microscopy, light-sheet microscopy and super-resolution microscopy, a hybrid system that harnesses the advantages of different designs will open new avenues to address biological problems.

Conflict of Interest

The authors declare no conflicts of interest.

Acknowledgments

This paper was supported by Shenzhen Science and Technology Innovation grants (JCYJ20200109 115633343, JCYJ20210324123610030).

References

1. L. Armbrecht, P. S. Dittrich, "Recent advances in the analysis of single cells," *Anal. Chem.* **89**(1), 2–21 (2017).
2. E. Lubeck, L. Cai, "Single-cell systems biology by super-resolution imaging and combinatorial labeling," *Nat. Methods* **9**(7), 743–748 (2012).
3. Y. Y. Hui, L.-J. Su, O. Y. Chen, Y.-T. Chen, T.-M. Liu, H.-C. Chang, "Wide-field imaging and flow cytometric analysis of cancer cells in blood by fluorescent nanodiamond labeling and time gating," *Sci. Rep.* **4**(1), 1–7 (2014).
4. A. Sharonov, R. M. Hochstrasser, Wide-field subdiffraction imaging by accumulated binding of diffusing probes, *Proc. Natl. Acad. Sci.* **103**(50), 18911–18916 (2006).
5. A. S. Stender *et al.*, "Single cell optical imaging and spectroscopy," *Chem. Rev.* **113**(4), 2469–2527 (2013).
6. S. Bohn *et al.*, "Cellular in vivo 3D imaging of the cornea by confocal laser scanning microscopy," *Biomed. Opt. Express* **9**(6), 2511–2525 (2018).
7. K. König, U. Simon, K. Halbhuber, "3D resolved two-photon fluorescence microscopy of living cells using a modified confocal laser scanning microscope," *Cell. Mol. Biol. (Noisy-le-grand)* **42**(8), 1181–1194 (1996).
8. K. Chatterjee, F. W. Pratiwi, F. C. M. Wu, P. Chen, B.-C. Chen, "Recent progress in light sheet microscopy for biological applications," *Appl. Spectrosc.* **72**(8), 1137–1169 (2018).
9. M. Weber, M. Mickoleit, J. Huisken, "Light sheet microscopy," *Methods Cell Biol.* **123**, 193–215 (2014).
10. M. Levoy, R. Ng, A. Adams, M. Footer, M. Horowitz, "Light field microscopy," *ACM Trans. Graph.* **25**, 924–934 (2006).
11. M. Levoy, Z. Zhang, I. McDowall, "Recording and controlling the 4D light field in a microscope using microlens arrays," *J. Microsc.* **235**(2), 144–162 (2009).
12. J. Kim, Y. Kim, Y. Jeong, B. Lee, A single-shot 2D/3D simultaneous imaging microscope based on light field microscopy, *Fifth Asia-Pacific Optical Sensors Conf.*, p. 96551O, International Society for Optics and Photonics (2015).
13. L. Galdón, G. Saavedra, J. Garcia-Sucerquia, M. Martínez-Corral, E. Sánchez-Ortiga, "Fourier lightfield microscopy: A practical design guide," *Appl. Optics* **61**(10), 2558–2564 (2022).
14. J. R. Bergen, E. H. Adelson, The plenoptic function and the elements of early vision, *Computational Models of Visual Processing*, Vol. 1, p. 8, MIT Press, US (1991).
15. M. Levoy, P. Hanrahan, Light field rendering, *Proc. 23rd Annual Conf. Computer Graphics and Interactive Techniques*, pp. 31–42 (1996).
16. N. Cohen, S. Yang, A. Andalman, M. Broxton, L. Grosenick, K. Deisseroth, M. Horowitz, M. Levoy, "Enhancing the performance of the light field microscope using wavefront coding," *Opt. Express* **22**(20), 24817–24839 (2014).
17. X. Lin, J. Wu, G. Zheng, Q. Dai, "Camera array based light field microscopy," *Biomed. Opt. Express* **6**(9), 3179–3189 (2015).
18. T. G. Georgiev, A. Lumsdaine, "Focused plenoptic camera and rendering," *J. Electron. Imag.* **19**(2), 021106 (2010).
19. J. Madrid-Wolff, M. Forero-Shelton, "Protocol for the design and assembly of a light sheet light field microscope," *Methods Protoc.* **2**(3), 56 (2019).
20. M. Broxton, L. Grosenick, S. Yang, N. Cohen, A. Andalman, K. Deisseroth, M. Levoy, "Wave optics theory and 3-D deconvolution for the light field microscope," *Opt. Express* **21**(21), 25418–25439 (2013).
21. A. Llavador, J. Sola-Pikabea, G. Saavedra, B. Javidi, M. Martínez-Corral, "Resolution improvements in integral microscopy with Fourier plane recording," *Opt. Express* **24**(18), 20792–20798 (2016).
22. C. Guo, W. Liu, X. Hua, H. Li, S. Jia, "Fourier lightfield microscopy," *Opt. Express* **27**(18), 25573–25594 (2019).

23. Z. Zhang, L. Bai, L. Cong, P. Yu, T. Zhang, W. Shi, F. Li, J. Du, K. Wang, "Imaging volumetric dynamics at high speed in mouse and zebrafish brain with confocal light field microscopy," *Nat. Biotechnol.* **39**(1), 74–83 (2021).
24. M. A. Taylor, T. Nöbauer, A. Pernia-Andrade, F. Schlumm, A. Vaziri, "Brain-wide 3D light-field imaging of neuronal activity with speckle-enhanced resolution," *Optica* **5**(4), 345–353 (2018).
25. T. Georgiev, A. Lumsdaine, The multifocus plenoptic camera, *Digital Photography VIII*, p. 829908, International Society for Optics and Photonics (2012).
26. L. Cong, Z. Wang, Y. Chai, W. Hang, C. Shang, W. Yang, L. Bai, J. Du, K. Wang, Q. Wen, Rapid whole brain imaging of neural activity in freely behaving larval zebrafish (Danio rerio), *Elife* **6**, e28158 (2017).
27. A. Stefanoiu, J. Page, P. Symvoulidis, G. G. Westmeyer, T. Lasser, Artifact-free deconvolution in light field microscopy, *Opt. Express* **27**(22), 31644–31666 (2019).
28. M. Zhang, Z. Geng, R. Pei, X. Cao, Z. Zhang, "Three-dimensional light field microscope based on a lenslet array," *Opt. Commun.* **403**, 133–142 (2017).
29. T. Georgiev, A. Lumsdaine, Superresolution with plenoptic camera 2.0, Adobe Systems Incorporated, Technical Report (2009).
30. H. Li, C. Guo, S. Jia, High-resolution light-field microscopy, in *Frontiers in Optics 2017* (Optica Publishing Group, 2017), p. FW6D.3.
31. H. Li *et al.*, "Fast, volumetric live-cell imaging using high-resolution light-field microscopy," *Biomed. Opt. Express* **10**(1), 29–49 (2019).
32. B. Mandracchia, X. Hua, C. Guo, J. Son, T. Urner, S. Jia, "Fast and accurate sCMOS noise correction for fluorescence microscopy," *Nat. Commun.* **11**(1), 1–12 (2020).
33. Y. Chen, B. Xiong, Y. Xue, X. Jin, J. Greene, L. Tian, "Design of a high-resolution light field miniscope for volumetric imaging in scattering tissue," *Biomed. Opt. Express* **11**(3), 1662–1678 (2020).
34. W. Liu, S. Jia, "wFLFM: enhancing the resolution of fourier light-field microscopy using a hybrid wide-field image," *Appl. Phys. Express* **14**(1), 012007 (2021).
35. X. Hua, W. Liu, S. Jia, "High-resolution Fourier light-field microscopy for volumetric multi-color live-cell imaging," *Optica* **8**(5), 614–620 (2021).
36. J. Drost, H. Clevers, "Organoids in cancer research," *Nat. Rev. Cancer* **18**(7), 407–418 (2018).
37. W. Liu, G.-A. R. Kim, S. Takayama, S. Jia, Fourier light-field imaging of human organoids with a hybrid point-spread function, *Biosens. Bioelectron.* **208**, 114201 (2022).
38. J. Wu *et al.*, "Iterative tomography with digital adaptive optics permits hour-long intravital observation of 3D subcellular dynamics at millisecond scale," *Cell* **184**(12), 3318–3332 (2021).
39. D. E. Milkie, E. Betzig, N. Ji, "Pupil-segmentation-based adaptive optical microscopy with full-pupil illumination," *Opt. Lett.* **36**(21), 4206–4208 (2011).
40. L. Ma, Y. Li, J. Peng, D. Wu, X. Zhao, Y. Cui, L. Chen, X. Yan, Y. Du, L. Yu, "Discovery of the migrasome, an organelle mediating release of cytoplasmic contents during cell migration," *Cell Res.* **25**(1), 24–38 (2015).
41. B. Xiong *et al.*, "Mirror-enhanced scanning light-field microscopy for long-term high-speed 3D imaging with isotropic resolution," *Light Sci. Appl.* **10**(1), 1–11 (2021).
42. N. Wagner, N. Norlin, J. Gierten, G. de Medeiros, B. Balázs, J. Wittbrodt, L. Hufnagel, R. Prevedel, "Instantaneous isotropic volumetric imaging of fast biological processes," *Nat. Methods* **16**(6), 497–500 (2019).
43. G. D. Medeiros, N. Norlin, S. Gunther, M. Albert, L. Panavaite, U.-M. Fiuza, F. Peri, T. Hiiragi, U. Krzic, L. Hufnagel, "Confocal multiview light-sheet microscopy," *Nat. Commun.* **6**(1), 1–8 (2015).
44. J. M. Wolff, D. Castro, P. Arbeláez, M. Forero-Shelton, Light-sheet enhanced resolution of light field microscopy for rapid imaging of large volumes, *Three-dimensional and Multidimensional Microscopy: Image Acquisition and Processing XXV*, p. 104991U, International Society for Optics and Photonics (2018).
45. D. Wang, S. Xu, P. Pant, E. Redington, S. Soltanian-Zadeh, S. Farsiu, Y. Gong, "Hybrid light-sheet and light-field microscope for high resolution and large volume neuroimaging," *Biomed. Opt. Express* **10**(12), 6595–6610 (2019).
46. I. V. Larina, S. Ivers, S. Syed, M. E. Dickinson, K. V. Larin, "Hemodynamic measurements from individual blood cells in early mammalian embryos with Doppler swept source OCT," *Opt. Lett.* **34**(7), 986–988 (2009).
47. T. P. Santisakultarm, C. J. Kersbergen, D. K. Bandy, D. C. Ide, S.-H. Choi, A. C. Silva, "Two-photon imaging of cerebral hemodynamics and neural activity in awake and anesthetized marmosets," *J. Neurosci. Methods* **271**, 55–64 (2016).
48. T. V. Truong, D. B. Holland, S. Madaan, A. Andreev, K. Keomanee-Dizon, J. V. Troll, D. E. Koo, M. J. McFall-Ngai, S. E. Fraser, "High-contrast, synchronous volumetric imaging with selective volume illumination microscopy," *Commun. Biol.* **3**(1), 1–8 (2020).

49. S. Madaan, K. Keomanee-Dizon, M. Jones, C. Zhong, A. Nadtochiy, P. Luu, S. E. Fraser, T. V. Truong, "Single-objective selective-volume illumination microscopy enables high-contrast light-field imaging," *Opt. Lett.* **46**(12), 2860–2863 (2021).
50. J. M. Taylor, C. D. Saunter, G. D. Love, J. M. Girkin, D. J. Henderson, B. Chaudhry, "Real-time optical gating for three-dimensional beating heart imaging," *J. Biomed. Opt.* **16**(11), 116021 (2011).
51. Z. Wang, Y. Ding, S. Satta, M. Roustaei, P. Fei, T. K. Hsiai, "A hybrid of light-field and light-sheet imaging to study myocardial function and intracardiac blood flow during zebrafish development," *PLOS Comput. Biol.* **17**(7), e1009175 (2021).
52. Y. M. Sigal, R. Zhou, X. Zhuang, "Visualizing and discovering cellular structures with super-resolution microscopy," *Science* **361**(6405), 880–887 (2018).
53. A. G. Godin, B. Lounis, L. Cognet, "Super-resolution microscopy approaches for live cell imaging," *Biophys. J.* **107**(8), 1777–1784 (2014).
54. H. Feng, X. Wang, Z. Xu, X. Zhang, Y. Gao, "Super-resolution fluorescence microscopy for single cell imaging," *Adv. Exp. Med. Biol.* **1068**, 59–71 (2018).
55. M. Saxena, G. Eluru, S. S. Gorthi, "Structured illumination microscopy," *Adv. Opt. Photon.* **7**(2), 241–275 (2015).
56. D. Wang, S. Roy, A. M. Rudzite, G. D. Field, Y. Gong, "High-resolution light-field microscopy with patterned illumination," *Biomed. Opt. Express* **12**(7), 3887–3901 (2021).
57. Z. Fu, Q. Geng, J. Chen, L.-A. Chu, A.-S. Chiang, S.-C. Chen, "Light field microscopy based on structured light illumination," *Opt. Lett.* **46**(14), 3424–3427 (2021).
58. R. R. Sims *et al.*, "Single molecule light field microscopy," *Optica* **7**(9), 1065–1072 (2020).
59. W. C. Lemon, K. McDole, "Live-cell imaging in the era of too many microscopes," *Curr. Opin. Cell Biol.* **66**, 34–42 (2020).
60. M. Levoy, "Light fields and computational imaging," *Computer* **39**(8), 46–55 (2006).
61. H. Zhu, Q. Wang, J. Yu, "Light field imaging: models, calibrations, reconstructions, and applications," *Front. Inform. Tech. El.* **18**(9), 1236–1249 (2017).
62. Y. Zhang, H. Lv, Y. Liu, H. Wang, X. Wang, Q. Huang, X. Xiang, Q. Dai, "Light-field depth estimation via epipolar plane image analysis and locally linear embedding," *IEEE Trans. Circuits Syst. Video Technol.* **27**(4), 739–747 (2016).
63. M. W. Tao, S. Hadap, J. Malik, R. Ramamoorthi, Depth from combining defocus and correspondence using light-field cameras, *Proc. IEEE Int. Conf. Computer Vision*, pp. 673–680 (2013).
64. D. Liang, X. Peng, Y. Hu, F. Zhao, S. Zheng, G. Situ, J. Liu, "Light-sheet light-field fluorescence microscopy," *Opt. Laser Eng.* **153**, 107015 (2022).
65. M. Shaw, H. Zhan, M. Elmi, V. Pawar, C. Essmann, M. A. Srinivasan, "Three-dimensional behavioural phenotyping of freely moving C. elegans using quantitative light field microscopy," *PLOS ONE* **13**(7), e0200108 (2018).
66. P. Sarder, A. Nehorai, "Deconvolution methods for 3-D fluorescence microscopy images," *IEEE Signal Process Mag.* **23**(3), 32–45 (2006).
67. D. Sage, L. Donati, F. Soulez, D. Fortun, G. Schmit, A. Seitz, R. Guiet, C. Vonesch, M. Unser, "DeconvolutionLab2: An open-source software for deconvolution microscopy," *Methods* **115**, 28–41 (2017).
68. R. Prevedel *et al.*, "Simultaneous whole-animal 3D imaging of neuronal activity using light-field microscopy," *Nat. Methods* **11**(7), 727–730 (2014).
69. P. Quicke, C. L. Howe, P. Song, H. V. Jadan, C. Song, T. Knöpfel, M. Neil, P. L. Dragotti, S. R. Schultz, A. J. Foust, "Subcellular resolution three-dimensional light-field imaging with genetically encoded voltage indicators," *Neurophotonics* **7**(3), 035006 (2020).
70. Y. Sung, "Snapshot projection optical tomography," *Phys. Rev. Appl.* **13**(5), 054048 (2020).
71. Q. Zheng, X. Jin, Y. Chen, Design of a light field microscope with uniform spatial resolution across an extended 3D volume, *Optical Design and Testing XI*, pp. 99–111, SPIE (2021).
72. J. Wu, B. Xiong, X. Lin, J. He, J. Suo, Q. Dai, "Snapshot hyperspectral volumetric microscopy," *Sci. Rep.* **6**(1), 1–10 (2016).
73. L. A. Shepp, Y. Vardi, Maximum likelihood reconstruction for emission tomography, *IEEE Trans. Med. Imag.* **1**(2), 113–122 (1982).
74. M. Yan, J. Chen, L. A. Vese, J. Villasenor, A. Bui, J. Cong, EM+ TV based reconstruction for cone-beam CT with reduced radiation, *Int. Symp. Visual Computing*, pp. 1–10. Springer (2011).
75. A. Stefanoiu, G. Scrofani, G. Saavedra, M. Martínez-Corral, T. Lasser, 3d deconvolution in fourier integral microscopy, in *Computational Imaging V*, p. 113960I, International Society for Optics and Photonics (2020).
76. P. J. Green, "On use of the EM algorithm for penalized likelihood estimation," *J. R. Stat. Soc. B* **52**(3), 443–452 (1990).
77. H. Verinaz-Jadan, P. Song, C. L. Howe, A. J. Foust, P. L. Dragotti, Volume reconstruction for light field microscopy, in *ICASSP 2020-2020 IEEE Int. Conf. Acoustics, Speech and Signal Processing (ICASSP)*, pp. 1459–1463, IEEE (2020).

78. L. Donati, E. Soubies, M. Unser, Inner-loop-free admm for cryo-em, *2019 IEEE 16th Int. Symp. Biomedical Imaging (ISBI 2019)*, pp. 307–311, IEEE (2019).
79. T. Rasal, T. Veerakumar, B. N. Subudhi, S. Esakkirajan, "Mixed poisson gaussian noise reduction in fluorescence microscopy images using modified structure of wavelet transform," *IET Image Proc.* **15**(7), 1383–1398 (2021).
80. N. C. Pégard, H.-Y. Liu, N. Antipa, M. Gerlock, H. Adesnik, L. Waller, "Compressive light-field microscopy for 3D neural activity recording," *Optica* **3**(5), 517–524 (2016).
81. T. Nöbauer, O. Skocek, A. J. Pernia-Andrade, L. Weilguny, F. M. Traub, M. I. Molodtsov, A. Vaziri, Video rate volumetric Ca^{2+} imaging across cortex using seeded iterative demixing (SID) microscopy, *Nat. Methods* **14**(8), 811–818 (2017).
82. Y.-G. Yoon *et al.*, Sparse decomposition light-field microscopy for high speed imaging of neuronal activity, *Optica* **7**(10), 1457–1468 (2020).
83. Z. Lu, J. Wu, H. Qiao, Y. Zhou, T. Yan, Z. Zhou, X. Zhang, J. Fan, Q. Dai, "Phase-space deconvolution for light field microscopy," *Opt. Express* **27** (13), 18131–18145 (2019).
84. Z. Zhang, Y. Liu, Q. Dai, Light field from micro-baseline image pair, *Proc. IEEE Conf. Computer Vision and Pattern Recognition*, pp. 3800–3809 (2015).
85. R. Keys, "Cubic convolution interpolation for digital image processing," *IEEE Trans. Acoust. Speech Signal Process.* **29**(6), 1153–1160 (1981).
86. S. Gu, L. Zhang, W. Zuo, X. Feng, Weighted nuclear norm minimization with application to image denoising, *Proc. IEEE Conf. Computer Vision and Pattern Recognition*, pp. 2862–2869 (2014).
87. J. He, Y. Cai, J. Wu, Q. Dai, "Spatial-temporal low-rank prior for low-light volumetric fluorescence imaging," *Opt. Express* **29**(25), 40721–40733 (2021).
88. H.-Y. Liu, E. Jonas, L. Tian, J. Zhong, B. Recht, L. Waller, 3D imaging in volumetric scattering media using phase-space measurements, *Opt. Express* **23**(11), 14461–14471 (2015).
89. Y. Zhang *et al.*, "Computational optical sectioning with an incoherent multiscale scattering model for light-field microscopy," *Nat. Commun.* **12**(1), 1–11 (2021).
90. L. Zhu, C. Yi, G. Li, Y. Zhao, P. Fei, Deep-learning based dual-view light-field microscopy enabling high-resolution 3D imaging of dense signals, *Bio-Optics: Design and Application*, pp. DTh2A–3, Optical Society of America (2021).
91. P. Song, H. V. Jadan, C. L. Howe, P. Quicke, A. J. Foust, P. L. Dragotti, Model-inspired deep learning for light-field microscopy with application to neuron localization, *ICASSP 2021-2021 IEEE Int. Conf. Acoustics, Speech and Signal Processing (ICASSP)*, pp. 8087–8091, IEEE (2021).
92. X. Li, H. Qiao, J. Wu, Z. Lu, T. Yan, R. Zhang, X. Zhang, Q. Dai, DeepLFM: Deep learning-based 3D reconstruction for light field microscopy, *Novel Techniques in Microscopy*, pp. NM3C–2, Optical Society of America (2019).
93. Ö. Çiçek, A. Abdulkadir, S. S. Lienkamp, T. Brox, O. Ronneberger, 3D U-Net: learning dense volumetric segmentation from sparse annotation, *Int. Conf. Medical Image Computing and Computer-assisted Intervention*, pp. 424–432, Springer (2016).
94. Z. Wang *et al.*, "Real-time volumetric reconstruction of biological dynamics with light-field microscopy and deep learning," *Nat. Methods* **18**(5), 551–556 (2021).
95. J. P. Vizcaino, F. Saltarin, Y. Belyaev, R. Lyck, T. Lasser, P. Favaro, "Learning to reconstruct confocal microscopy stacks from single light field images," *IEEE Trans. Comput. Imag.* **7**, 775–788 (2021).
96. Y. Zhang, B. Xiong, Y. Zhang, Z. Lu, J. Wu, Q. Dai, "DiLFM: An artifact-suppressed and noise-robust light-field microscopy through dictionary learning," *Light Sci. Appl.* **10**(1), 1–12 (2021).